Proceedings of the NYU Tandon School of Engineering
Mechanical & Aerospace Engineering Department
ME-UY 4113 Senior Design II Section A
Spring 2026, Brooklyn, NY, USA

Climbing Robots for Construction
Team: Climbing Clankers

Yupeng Li	yl11710@nyu.edu
Henry Elliott	he2102@nyu.edu
Melanie Lin	ml8820@nyu.edu
Jonathan Shan	jes9899@nyu.edu
Tahasin Iqbal	tji8225@nyu.edu

NYU Tandon School of Engineering, B.S. in Mechanical Engineering, Brooklyn, NY

ABSTRACT

This project aims to develop a climbing robotic system that automates the vertical assembly of steel columns using bolted splice plates. Currently, ironworkers manually align columns and install bolts at significant heights, exposing them to fall hazards, suspended loads, and heavy equipment. To address this problem, an autonomous robot capable of climbing an I-beam, positioning itself at the connection interface, aligning pre-placed plates, and tightening bolts with controlled torque was designed. The system integrates a spring-loaded wheel locomotion mechanism, a dual-spindle fastening tool for simultaneous bolt tightening, and a plate-handling subsystem powered by passive springs for energy efficiency. Sensing is achieved using motor encoders, photoelectric sensors, and torque feedback to ensure accurate positioning and prevent bolt stripping.

NOMENCLATURE

V	Bus Voltage (V)
I	Operating Current (A)
Ipeak	Peak Current (A)
P	Electrical Power (W)
t	Operating Time (hr)
Wh	Energy Consumption (W*hr)
Ah	Operating Current (A*hr)
F	Force (lbf)
k	Spring Stiffness (lbf/in)
x	Spring Displacement (in)
μf	Coefficient of Friction
W	Robot Weight (lbf)
FOS	Factor of Safety
n	Number of Wheels
T	Torque (N*m)
r	Radius of Wheel (m)

1. INTRODUCTION

1.1 Problem Definition

Steel column assembly remains one of the most dangerous tasks in the construction industry. Ironworkers must manually position splice plates, align two vertical columns, and tighten bolts while balancing on narrow flanges and working near suspended members. These operations introduce high risks of falls, dropped tools, and crush injuries. According to the Bureau of Labor Statistics, ironworking is among the top 10 most dangerous jobs in the U.S., with construction accounting for 1,075 of 5,283 occupational fatalities in 2023 [1]. As demand for faster and safer construction grows, there is a clear market need for automation that can reduce human exposure to these hazardous tasks.

Despite significant advancements in robotics for manufacturing and logistics, construction sites still rely heavily on manual assembly. The harsh, unstructured environment presents unique challenges for automation, including variable tolerances, irregular surfaces, and environmental contamination. This gap represents a significant opportunity to introduce an integrated robotic solution that enhances jobsite safety, improves connection reliability, and increases productivity.

© 2026 by CLIMBING CLANKERS

The project addresses this challenge by developing an autonomous climbing robot capable of ascending a vertical steel column and performing a complete bolted splice-plate connection. The design aims to apply core mechanical principles of traction and clamping–including spring-loaded wheel modules for reliable grip on I-beam webs–a dual-spindle bolting assembly for simultaneous fastening, and a passive plate-handling mechanism. A mechatronic design methodology was adopted by integrating sensing, actuation, and control to achieve autonomous hole detection and torque regulation.

The major assumptions for the solution include the use of a 6061-T6 aluminum I-beam as a prototyping surrogate for steel, the pre-positioning of columns by a crane, and compliance with standard AISC bolted connection practices [2].

The key measurable specs that the robot shall achieve are a stable vertical climbing at a speed ≥ 0.15 m/s with a minimum factor of safety ≥ 2 against slip; plate and bolt hole alignment within a tolerance of ±2 mm; bolt tightening to a target torque of 8–12 Nm (snug-tight), with a hard limit of 16 Nm; a bolting cycle time of < 8 seconds per bolt; integration of all subsystems into a fully functional, portable prototype with a total mass < 25 kg. These requirements guide the full system design, analysis, and development of a functional prototype.

1.2 Prior Art

Numerous climbing robots have been developed for inspection or maintenance, but few address structural assembly. Background research reveals that while climbing robots and automated bolting systems exist independently, a system integrating both functions for on-site steel assembly is novel.

A common approach for vertical mobility is suction-based adhesion, as seen in the modular robot patented by Sadegh and Xiao [3]. While capable of traversing smooth walls, such systems are power-intensive and perform poorly on the rough, dirty, or painted surfaces typical in construction. An alternative is magnetic adhesion, exemplified by the adjustable wheel-spacing climber described in a recent patent by Liu et al. [4], which is more suitable for ferrous structures like steel columns. Video demonstrations, such as the compact wheel-based climber from Missouri S&T, confirm the feasibility of mechanical traction for lightweight inspection robots [5].

Some other adhesion methods commonly employed include adhesive adhesion, claw grasping, electrostatic absorption, clamping adhesion, and hybrid adhesion which combines the above types together [6]. One example of hybrid adhesion is the climbing robot developed by Ko et al. which uses a combination of static electricity, rubber adhesion, and tail forces through a torsional spring, as inspired by the climbing mechanism of geckos [7]. The electrostatic adhesion is enhanced by the elastomer (i.e. rubber) and flexible material which acts as a dielectric to resist peeling force. The robot also uses a track structure to implement the adhesion methods stated above. Such a hybrid engineering approach may increase complexity, but also provides the most optimal configuration for achieving adhesion in climbing robots and can be applied to similar projects.

An interesting example of hybrid adhesion is the combination of the clamping and adhesive absorption methods to grip onto beams and poles, as demonstrated by Liu and Padrigalan [8]. The design involves spring-loaded wheels which clamp onto the surface, with the wheels also being made of an elastic material that provides a sufficient coefficient of friction between the wheel tires and contact surface. The robot achieved an average speed of 120 mm/s, which was a promising result to warrant a similar design to be explored in this project.

Besides adhesion, there have been various types of locomotion methods developed for climbing robots as well. One approach is the use of legged locomotion, as seen in the four-legged robot, LEMUR 3, developed by Parness et al [9]. Legged robots are more complicated to design and control, especially when it comes to climbing vertical surfaces, however they also offer increased adaptability. Some other locomotion types include wheeled, tracked, rope-driven, and inchworm locomotion [6]. Again, like with the adhesion methods, there is also a hybrid locomotion style describing robots that combine different types of locomotion.

Wheeled locomotion offers several advantages in that it offers fast and continuous movement, a simple structure, simple control, and low-energy consumption in comparison to the other locomotion styles. An example of a climbing robot that uses wheeled locomotion is the UT-PCR developed by Ahmadabadi et al [10]. The robot consists of a triangular body with three limbs and wheels that are spaced 120º apart. The wheels are spring loaded, resulting in a clamping force that grips around the pole. In the text, the wheels are said to be nonholonomic, which means that the wheels are unable to slip sideways. These become nonholonomic constraints that make the system underactuated, where the three wheels are used to control a 6-DOF system. The authors found three basic motion primitives that fully control the nonholonomic robot: position tracking, vertical alignment, and rotation around the pole. The kinematic model and control method that were derived can be applied to similar cases.

Automated bolting technology is well-established in controlled factory settings. For instance, Volvo's patented robotic tightening tool employs a self-centering mechanism to ensure repeatable torque application [11]. Within construction automation research, Nam et al. developed a bolting robot that frames the task as a peg-in-hole alignment problem [12], while Chu et al. proposed a sophisticated dual-tool system for installing specialized tension-control bolts [13]. These systems

 © 2026 by CLIMBING CLANKERS

achieve high precision but are not designed for the payload, mobility, or environmental variability required for field deployment on climbing platforms.

Despite the progress around automated bolting methods and climbing robotics, the technologies have not been integrated into a single, field-deployable system for construction assembly. No system has combined both climbing, plate handling, and torque-controlled fastening. Additionally, current climbing mechanisms are only capable of supporting the weight of a robot plus potentially a small end-effector. In order to carry the weight and reaction forces of a bolting end-effector (e.g., powerful magnets), the climbing technology will need to become more heavy and complex. Finally, these developments have mainly occurred in academic and research environments, however these fail to consider real-world challenges like hole misalignment, surface debris, or vertical oscillation.

This project directly addresses these gaps by designing a cohesive system that combines a simple, reliable spring-wheel traction mechanism with a dedicated, torque-controlled bolting end-effector, creating a novel solution tailored for autonomous steel column assembly on construction sites.

2. REQUIREMENTS

2.1 Customer Needs

The two primary customers of this project are construction companies and the project's advisor, whose needs shape the design requirements of the project.

Construction companies require safer and more efficient methods to perform vertical steel column assembly. Their priorities include reducing worker exposure to hazardous heights, minimizing delays caused by manual bolting, and improving connection consistency and quality. Construction companies also demand equipment that is robust, portable, easy to deploy and handle, and compatible with standard steel structures used on job sites. A new type of automated technology that is to be integrated into the construction industry should also be simple enough for all workers to adapt to without sacrificing effectiveness.

As the academic advisor and evaluator of the project, Professor Ludovic Dominique Righetti provides additional performance criteria and research expectations for this project. His expertise in robotics, locomotion, and control informs the project's system-level requirements, such as reliability, safety considerations, feasibility of the locomotion strategy, and the integration of sensing and actuation–which may not be immediately available from the other customers' needs.
In summary, the main needs that project must address are enhancing worker safety by automating high-risk at-height bolting tasks, providing consistent, high-quality bolted connections that meet structural standards, achieving reliable and stable climbing on vertical steel I-beams, accurate alignment of splice plates with pre-drilled bolt holes, designing a portable, self-contained system that is practical for on-site deployment, and adhering to relevant electrical, mechanical, and industrial safety codes.

2.2 Target Specifications

Based on the customer needs, several engineering specifications and design constraints were established.

The geometry & structural specifications require the robotic system to be compatible with standard steel and the provided aluminum I-beam. The tolerances for flange thickness shall be within 0.330–0.370 in. The hole alignment accuracy is to be within 2 mm.

Below are the rest of the target specifications for each subsystem:

Locomotion
- Wheel traction coefficient: **≥ 0.5**
- Slip safety factor: **≥ 2**
- Climbing speed: **≥ 0.10 m/s**
- Total system mass: **< 25 kg (50 lb)**
- Payload capacity (tools + plate): **≥ 3 kg**

Plate Handling
- Carry at least one splice plate (consisting of two holes)
- Passive clamping mechanism
- Clearance-adjustable arms for climbing transition

Fastening System
- Torque output: **8–12 Nm** target
- Hard torque limit: **16 Nm**
- Cycle time: **< 8 seconds per bolt**
- Dual-spindle configuration preferred for stability
- Encoder and torque feedback for accuracy

Electrical & Energy
- 24 V lithium-ion battery pack
- Integrated BMS, fuses, breakers, and E-stop
- 24 V → 12 V / 5 V power conversion
- Maximum system voltage: **< 50 V**

Relevant Codes and Standards
The design takes into consideration the following standards and safety regulations:
- **ANSI/RIA R15.06** – Industrial robot safety
- **ISO 10218** – Safety requirements for industrial robots
- **ANSI/RIA R15.08** – Autonomous mobile robot behavior
- **ISO 13849** – Machine control functional safety
- **NFPA 70 / NEC** – Electrical safety
- **NFPA 79** – Industrial machinery wiring
- **UL 3100** – Safety for electrical equipment
- **OSHA 29 CFR 1926 & 1910** – Construction and general industry safety

© 2026 by CLIMBING CLANKERS

- **ASTM E2395** – Anchorage and fall-related performance

These standards guide the safe development of the robotic system, especially for climbing, fastening, electrical design, and on-site operation.

3. Product Design

The final design consists of (1) the fastening assembly, (2) 4 locomotion wheel assembly, (3) the frame, and (4) the electronics mounting plate (Figure 1)

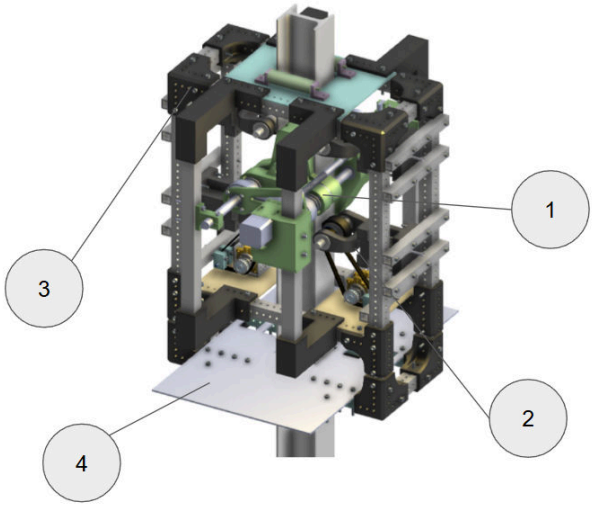


Figure 1: Top Level Assembly of Climbing Robot

The fastening assembly is responsible for positioning and driving the bolts during the automated fastening process. It contains the bolt-driving motors, fastening plate interface, and feed mechanism needed to move the fasteners toward the I-beam. The four locomotion wheel assemblies provide the robot's climbing motion and maintain contact with the beam through friction between the wheels and the aluminum surface. These wheel assemblies are mounted to the main frame, which serves as the structural backbone of the robot and supports all mechanical loads during climbing and fastening. Finally, the electronics mounting plate provides a centralized location for the Arduino, motor drivers, power distribution components, sensors, and wiring, allowing the control system to be organized, accessible, and protected during operation.

The operation process begins by vertically inserting the robot frame onto the I-beam through its center opening. The wheel modules are then secured to apply the required normal force against the beam, and the belt is tensioned to ensure proper traction during climbing. After the mechanical setup is complete, the fastening plate and nuts are manually loaded into the fastening assembly. Finally, the start button is activated, allowing the robot to begin its automated climbing and fastening sequence.

3.1 Theoretical Background

The design of the climbing construction robot is based on a combination of mechanical, electrical, and control system engineering principles. The primary theoretical foundations include traction and friction, structural mechanics, power transmission, and feedback control systems.

The locomotion system relies on friction-based climbing, where the available traction force must exceed the gravitational force acting on the robot.
Hooke's Law is applied to generate this normal force:

$$F_s = kx$$

This allows the system to maintain sufficient clamping force on the I-beam to prevent slip, while accommodating surface irregularities.

The fastening system is based on torque-controlled bolting mechanics, where proper bolt preload is achieved by controlling torque and rotation. The relationship between torque and bolt tension ensures structural integrity while avoiding over-tightening or stripping. Motor current is used as a proxy for torque, enabling a closed-loop control approach.
The structural design follows stress and deformation principles, ensuring that all components operate within material limits. Finite Element Analysis (FEA) was used to verify that stresses in the frame and wheel assembly remain below yield strength, achieving a high factor of safety.
Power transmission in the system uses belt and pulley mechanisms and gear reductions, which allow high torque output from compact motors. The torque relationship is:

$$T=Fr$$

where torque is generated through wheel radius and applied force.

Finally, the system integrates mechatronics and control theory, combining sensors (encoders, photoelectric sensors, current sensing) with actuators to achieve autonomous operation. Closed-loop feedback ensures accurate positioning, reliable climbing, and consistent bolt tightening.

3.2 Concept Development

3.2.1 Functional Decomposition

The system-level function of the robot is to attach a suspended and aligned aluminium column to a vertically secured column by autonomously transporting itself to the connection joint and performing a fastening operation (Figure 2).

© 2026 by CLIMBING CLANKERS

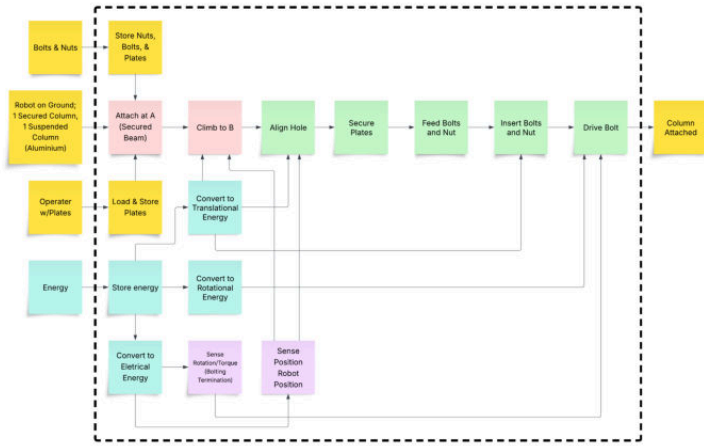


Figure 2: Functional Diagram of the Climbing Robot

As shown in the functional diagram, the robot can be decomposed into four primary subsystems: fastening (green), locomotion (red), energy (blue), and sensing (purple). The overall systematic operation begins with the robot being attached at the initial position on the secured column (A). The operator proceeds to load plates, bolts, and nuts required for fastening. The robot stores the loaded material and climbs to the jointed site between the suspended and secured column (B) and transitions into the fastening sequences: hole alignment, plate securing, bolts and nuts feeding and inserting, and bolt driving. The final achieved state is the successful attachment of the aluminium column.

Energy subsystems focus mainly on the storage and conversion of energy into the required forms of actuations: translation energy for the climbing, rotational energy for the bolt drives, and electrical energy for the sensors. The sensing subsystems provide closed loop feedback for the alignment and navigation, and the rotation/torque sensing determines tightening completion thus terminating the bolting.

3.2.2 Design Alternatives

Based on the functional decomposition, multiple solution concepts were brainstormed for each subsystem. These alternatives were then compared using performance criteria to justify the final concept selection.

3.2.3 Fastening

The primary fastening design decision was selecting a bolt-driving mechanism capable of securing the two-bolt plate at the joint. Three candidate concepts were brainstormed and are shown in Figure 3.

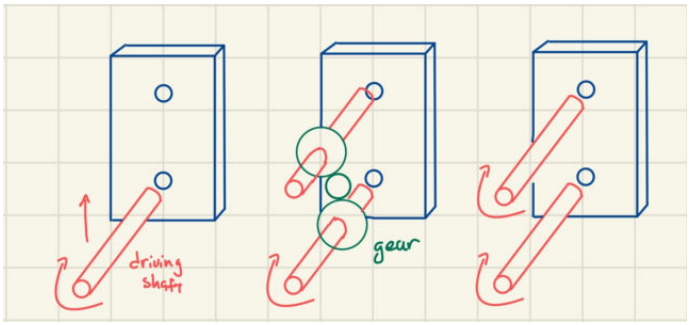


Figure 3: Bolt Driving Concepts for 2-hole Plate

From left to right of Figure 3, the bolt driving concepts considered were (1) a single moving spindle, where one driving shaft tightens one hole then the robot mechanically repositions itself to the second hole to tighten the other; (2) a single motor with a geared split, where one motor drives two output shafts through gears so both holes are covered but the two bolts are mechanically coupled; and (3) two independent spindles, where each hole has its own dedicated driving shaft (one motor each) so both bolts can be tightened with independent control. The functional notes for each of the concepts were noted in Table 1.

Table 1: Morphological Table of Bolt Driving Design

Function (Fastening)	**Moving Single Spindle**	**Gear-Split Two Spindle**	**Two Independent Spindles**
Reach both bolt locations	Linear repositioning	No repositioning	No repositioning
Tighten two bolts	Sequential	Simultaneous	Simultaneous
Control of each bolt	Same tool, same torque sensor	Coupled torque/speed between bolts	Independent torque/speed per bolt
Sensitivity to misalignment	High (must re-align after moving)	Low (Preposition by design)	Low (Preposition by design)
Mechanism complexity	Medium (needs moving stage + locking)	Medium–high (gearing + shaft routing)	Medium (two modules, simpler kinematics)

In comparison, design 1 utilizes a singular shaft to complete its bolting function. This creates simplicity in its primary function but adds complexity to the vertical control of the robot as the additional alignment adds potential for error. Design two removes the secondary alignment but introduces complexity in control as the system will be required to control fastening torque of two bolts based on one driving shaft. Design 3 removes the control complexity as it allows for independent control for each shaft but requires an additional motor, thus adding cost to the design. A scoring matrix with weight on the

© 2026 by CLIMBING CLANKERS

specific function on a scale from one to five is organized in Table 2 to finalize design choice.

Table 2: Scoring Matrix of Bolt Driving Design

Criteria	Weight	Moving Single Spindle	Gear-Split Two Spindle	Two Independent Spindles
Alignment	0.30	2	5	5
Torque ctrl	0.25	5	2	5
Cycle Time	0.25	2	4	5
Mechanical Simplicity	0.10	5	2	4
Mass	0.05	4	3	3
Cost	0.05	5	3	2
Total	**1.00**	**3.30**	**3.5**	**4.65**

For the scoring matrix in Table 2, greater weight was put on the actual function for the concept in the preliminary design stage (Alignment, torque control and cycle time). Ultimately design 3, two independent spindles were selected as the robust robustness for both alignment and cycle time it provides outweighs the drawback of additional cost.

The methods of how the bolting plate will be holed during the fastening process was also considered. Mainly two passive designs were brainstormed (Figure 4)

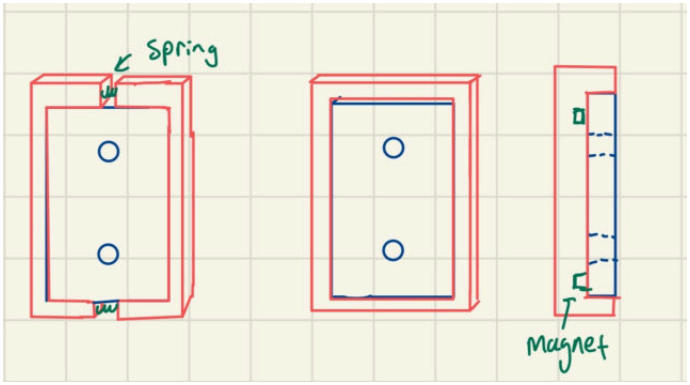


Figure 4: Passive Holding Concepts for 2-hole Plate

Because the two passive designs are relatively simple and have minimal cost differences (spring vs. magnet), design 2 (magnet) was ultimately selected for plate holding. It requires the least mechanical complexity while providing an additional factor of safety by enabling the plate to press-fit into the socket, improving retention during alignment and bolting.

The final preliminary design choice was to identify the method of linear motion between the bolt and the nut. Two design choices were considered, a dual threaded lead screw or two single threaded lead screws. Lead screw mechanisms are very common in machines which must perform exact linear motion and consist of an actuator, threaded shaft, nut(s) and a bearing block. A single lead screw design would be relatively complex, expensive for the project's scale, heavy, and associated with higher power draw. The main limiting factor is the moment introduced in the guides: because the lead screw would need to be placed outside the I-beam, an eccentric drive force would be created. This eccentricity increases the moment on the carriage, which in turn increases friction in the bearings and the load on the slides.

Ultimately the single lead screw mechanism was chosen. Because of the small geometric scale of the model and the modest speeds it will be required to move at moments will be kept to a minimum. The single lead screw also allows us to implement an easier control system as only one stepper needs to be controlled vs two being controlled synchronously. A single lead screw will also be cheaper, lighter, and consume less energy.

3.2.4 Locomotion

The primary design choice for locomotion was deciding the type of reliable contact/traction method for climbing along the column surface. Three different design options were brainstormed (Figure 5).

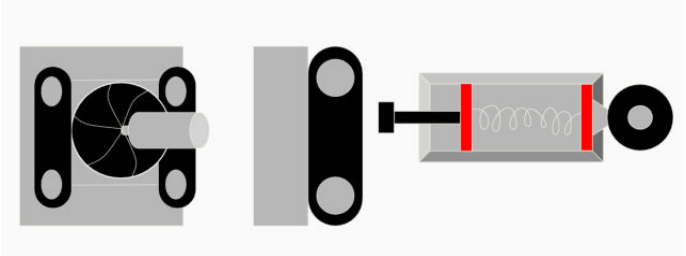


Figure 5: Locomotion Concept

From left to right of Figure 5, the wheel driving concepts considered were (1) spring-loaded wheels that apply adjustable normal force to clamp onto the beam; (2) tracked belt drive that increases contact area using a high-friction material to reduce slip and improve traction; and (3) suction-based adhesion that creates a pressure differential to generate suction force, with a DC motor providing the drive action. The functional notes for each of the concepts were noted in Table 3.

© 2026 by CLIMBING CLANKERS

Table 3: Morphological Table of Locomotion Design

Function (Fastening)	Spring Loaded Wheels	Track Drive	Suction Module
Provide normal force / adhesion	Adjustable spring clamp	Passive normal force + large contact area	Pressure differential (fan suction)
Generate upward motion	Two driven wheels	Driven track	Driven wheel(s) with suction holding
Slip resistance	Medium–high (depends on preload + μ)	High (large contact area + μ)	Variable (seal/surface dependent)
Compliance to surface variation	Good (spring compliance)	Good (wrap + compliance)	Lower (leaks reduce adhesion)
Mechanical complexity	Low	Medium	High (fan, sealing, ducting)
Power demand	Low–medium	Medium	High (continuous fan power)

In comparison, design 1 generates traction through an adjustable clamping force, providing a simple and power-efficient solution with good compliance to surface variation; however, its slip resistance depends strongly on the selected preload of the spring and the available friction coefficient. Design 2 increases contact area to improve slip resistance and stability, but introduces additional drivetrain complexity, geometry constraints, and higher power losses associated with belt/track mechanics. Concept 3 (suction module) replaces friction-based normal force with adhesion from a pressure differential, which can theoretically reduce reliance on surface friction, but requires continuous fan power and is more sensitive to sealing quality and surface condition, increasing complexity and risk. A scoring matrix with weight on the specific function on a scale from one to five is organized in Table 4 to finalize design choice.

Table 4: Scoring Matrix of Locomotion Design

Criteria	Weight	Spring-loaded wheels	Tracked drive	Suction module
Slip resistance	0.3	4	5	3
Robustness to Surface Vary	0.2	4	4	2
Power Cost	0.2	5	3	1
Integration	0.2	5	3	2
Mass	0.05	4	3	2
Cost	0.05	5	3	2
Total	**1**	**4.45**	**3.80**	**2.10**

For the scoring matrix in Table 4, greater weight was placed on the core locomotion requirements during the preliminary design stage: slip resistance, robustness to surface variation, power cost, and integration. This is because they directly translate to robots climbing capability and reliability. Ultimately, Concept 1 (spring-loaded wheels) was selected because its strong performance in traction reliability and system integration, combined with its low power demand and overall simplicity, outweighed the tracked drive's added mechanical complexity and the suction module's high power consumption and sensitivity to surface conditions.

3.2.4 Sensing, Control, and Energy

The primary sensing design decision for sensing was selecting a feedback method to support vertical alignment and hole detection during vertical climbing. Two candidate concepts were considered, motor encoder feedback and light-sensor detection (Figure 6).

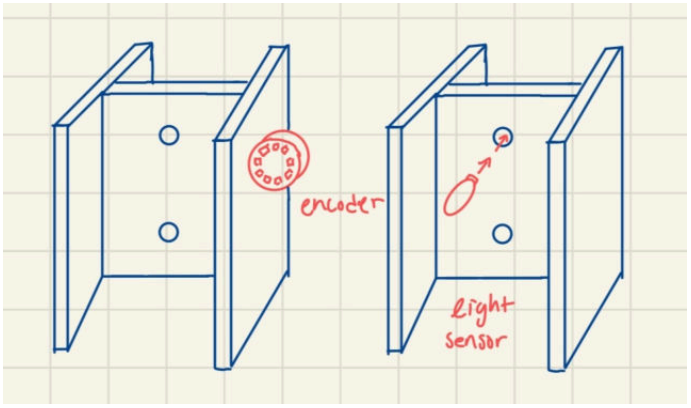


Figure 6: Locomotion Sensing Concept

From left to right in Figure 5, the sensing concepts considered were (1) motor encoder feedback, where the motor's rotation count is used to estimate vertical travel and provide fine incremental motion control near the joint; and (2) a light sensor, where local optical changes are used to detect hole presence (blocked/unblocked) and confirm entry/exit events for improved hole detection accuracy. The functional characteristics of each concept are summarized in Table 5.

Table 5: Morphological Table of Locomotion Sensing

Function (Sensing)	Motor Encoder	Light Sensor
Vertical alignment	Counts turns → rough vertical estimate	Local signals only
Hole detection	Can drift with slip	Detects hole blockage more accurately
Fine hole alignment	Oscillate/step around hole to converge	Flags entering/leaving hole
Environment robustness	Ignores light; affected by slip	Sensitive to ambient light; needs shielding
Integration	Built into motor	Requires added sensor + wiring

© 2026 by CLIMBING CLANKERS

In comparison, the motor encoder provides simple integration and allows for incremental control; but its vertical position estimate can drift due to wheel slip, which puts complexity against the millimeter-accuracy required by bolting hole alignment. However, since encoder-based vertical alignment is not strictly required because the robot climbs in incremental distances to the joint rather than relying on absolute height tracking, a light sensor can be used to indicate when the tool is approaching or passing a hole, thus signaling stop. This improves local hole detection; but it is more sensitive to environmental lighting and requires shielding to remain reliable. A scoring matrix with weight on the specific function on a scale from one to five is organized in Table 6 to finalize design choice.

Table 6: Scoring Matrix of Locomotion Sensing Design

Criteria	**Weight**	**Motor Encoder**	**Light Sensor**
Hole detection accuracy	0.35	3	5
Fine alignment capability	0.25	5	4
Robustness to environment	0.2	3	2
Integration simplicity	0.2	5	3
Total	**1**	**3.9**	**3.95**

For the scoring matrix in Table 6, greater weight was placed on hole detection accuracy and fine alignment capability, since these directly affect successful bolt insertion and fastening at the joint. Ultimately, the design selection uses both sensors in a complementary manner: the light sensor provides reliable local detection for rough alignment and hole finding, while the motor encoder is used primarily for controlled incremental motion during fine alignment, without relying on encoder counts as an absolute vertical position reference.

The sensing method for the fastening process was also considered. The design goal is a reliable control feedback loop for the bolt shaft motor to tighten the bolts. The ideation was based on the torque versus rotation plot of a general bolting tightening process (Figure 7).

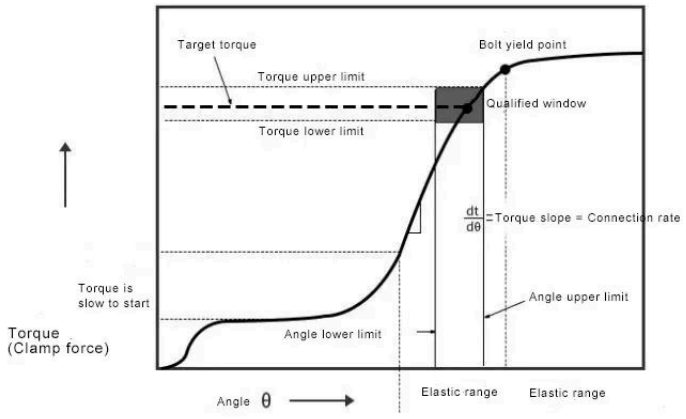


Figure 7: Torque Versus Rotation Angle Plot of General Bolt Tightening Process (Reproduced from [13])

To ensure the two spindle drive systems reach the qualified tightening window shown in Figure 6, each spindle can be controlled with a two-signal feedback loop: motor current (as a proxy for applied torque) and shaft rotation from an encoder (for angle/turn counting). In operation, each motor first runs in a speed-controlled phase until the bolt is seated, then transitions to a tightening phase where the controller monitors the rise in estimated torque (from current) versus rotation; tightening is terminated when the bolt enters the qualified torque band and meets a minimum additional angle after snugging. Because the robot uses two independent spindles, this logic can be applied independently to each bolt, allowing one spindle to stop at target while the other continues tightening until it also reaches the qualified window.

The primary energy design decision was selecting a method to store and deliver electrical power for all actuation and sensing needs, since the robot must convert stored energy into the required forms for climbing, clamping, and bolting. Two supply approaches were considered: wired power and battery power (Table 7).

Table 7: Morphological Table Power Supply

Criteria	**Wired**	**Battery**
Weight	Lighter / minimal onboard mass	Heavier and bulkier
Power	High / not limited by onboard capacity	Limited power relative to size
Practicality	Significantly limits movement (tether risk)	High mobility (untethered)

In comparison, a wired supply offers lower onboard weight and can provide effectively unlimited power. But the tether significantly limits robot movement and introduces a major snag/drag risk for a vertical climbing system. A battery-based supply is heavier and bulkier and its available power is limited by pack size, but it enables fully untethered operation and is therefore far more practical for reliable climbing and real-world deployment. Based on the emphasis on mobility and operational practicality, the battery-based electrical supply was selected despite the weight penalty.

3.3 Detailed Design

3.3.1 Fastening Assembly

3.3.1.1 Nut and Bolt Carriage

Based on the preliminary design choices (dual spindle, magnetic plate attachment, and dual lead screw), the bolt carriage provides the most crucial function of the system (Figure 8).

© 2026 by CLIMBING CLANKERS

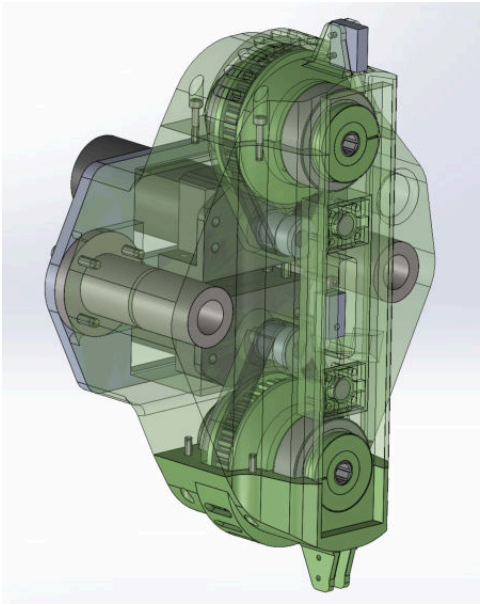


Figure 8: Nut Carriage Design

The required motor power to drive the bolts was first determined. The torque needed to secure the selected M5 nuts was taken as 13 ft·lbf. A minimum speed requirement of 15 rpm at the maximum torque value and a factor of safety of 2 were then assumed. This resulted in a minimum required motor power of 72.4 W. A 200 W motor was selected for the bill of materials, which exceeds the minimum requirement and includes an integrated planetary gearbox to increase available torque. Due to the limited width of the I-beam and the need for high torque output, belt drives were selected to couple the motor spindle to the bolt spindle.

The bolt spindle wall thickness was sized relative to another socket wrench head [14] with a factor of safety of 1.05 applied resulting in a minimum outer diameter of 0.77 in. This factor of safety is relatively low as the manufacturer has already applied their own factor of safety. The spindle diameter selected needs to then fit a bearing. The smallest common bearing size that met this criterion was a 20mm (0.79in) bore shaft bearing.

The 6204-2RS bearing was selected to support the spindle. After selection the bearing must meet the thrust, and radial loads of the design. SKF's recommended thrust criteria for deep groove ball bearings was used.

$$F_T \leq 0.25 C_o, C_o = 1472\ lbf, F_T \leq 370\ lbf \qquad (1)$$

This thrust load capacity far exceeds the capacity needed for the bolting process.

After identifying many design needs from the nut carriage the bolt carriage was designed. One of the project advisors Professor Debra Laefer suggested attaching the bolts directly to the plates to reduce the complexity of the project. This benefits design simplification greatly.

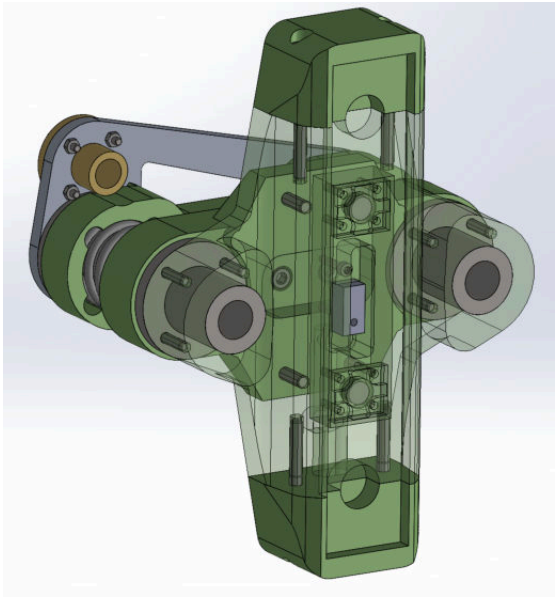


Figure 9: Bolt Carriage Design

The primary functions are to support the plate, hole detection, and force absorption. This force absorption is to account for the alignment failures which are likely to occur at our budget.

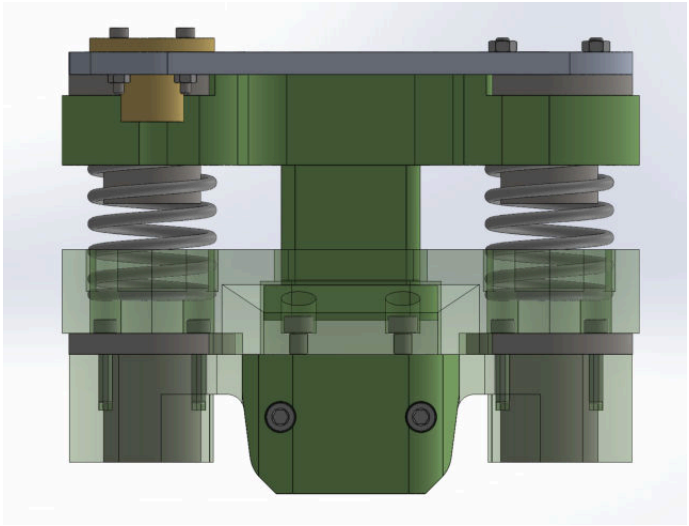


Figure 10: Spring Absorption Mechanism

As seen from above there is a physical range limiter between two intersecting parts which not only limits compression on the springs but also creates a small pretension.

Each of these carriages contain a small rectangular insert which houses magnets, a photo electric emitter, and a photo electric receiver. This was designed to be modular due to the difficulty of magnetic force calculations. This design allowed for iteration to find the ideal magnetic force for the plate securement.

© 2026 by CLIMBING CLANKERS

3.3.1.2 Carriages and Lead Screw

The bolt and nut carriages will be moved toward each other using a dual threaded lead screw powered by a stepper motor which attaches via a shaft coupling as seen in Figure 11. The stepper motor will provide a simple feedforward control system with a large degree of accuracy. The threads of the lead screw selected will have a 3mm pitch rotated at 1.8 degrees per step; the lead screw should provide a linear step of 0.015mm allowing for precise motion. Further system analysis will be required to determine the stepper motor torque and power requirements, but the preliminary design uses a 5V NEMA 17 stepper motor.

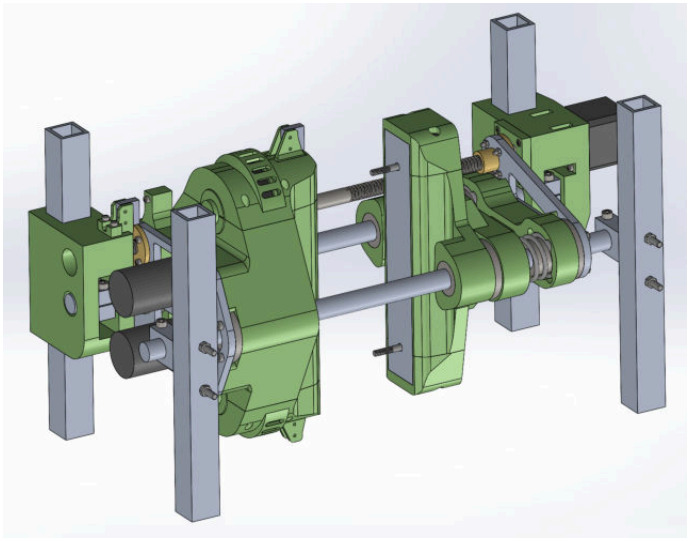


Figure 11: Fastening Subassembly

Given the 3mm pitch of the dual lead screw along with the 0.8mm pitch of the m5 bolt a feed rotation rate ratio was identified as 7.5.

To identify the needed stepper motor requirements and structural support a simplified model was used to identify the dynamic characteristics of the design.

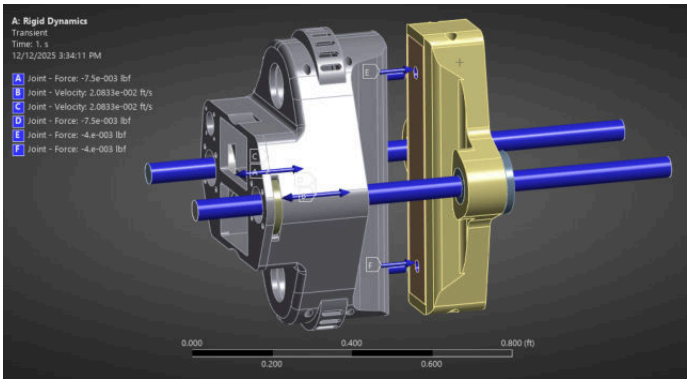


Figure 12: Rigid Dynamics

The simplified model was first simulated with rigid dynamics to establish the kinematic relationships between the lead screws constant velocity, the threading forces, and spring forces.

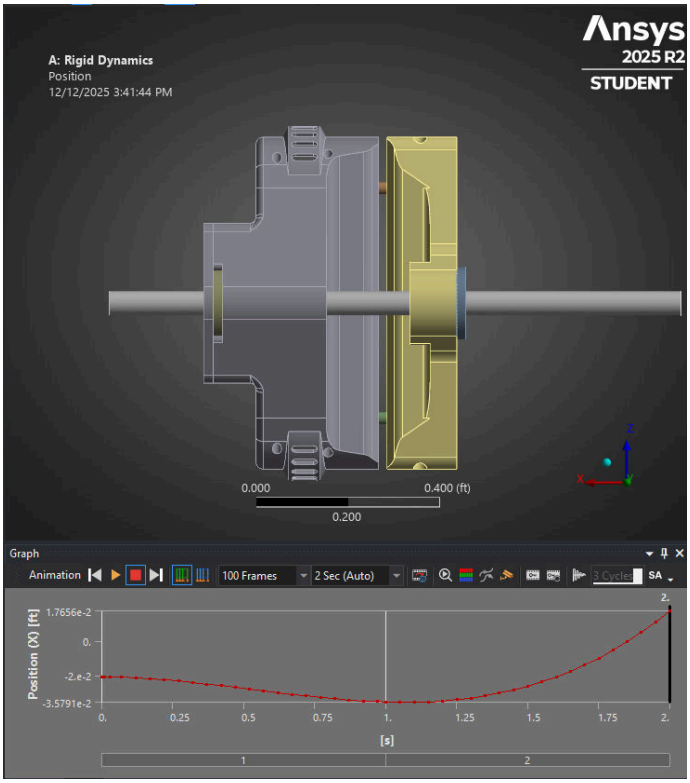


Figure 13: Rigid Dynamic of Design

The plot in Figure 13 shows the position along the x axis of the nut carriage over the bolting process. The nut carriage starts by slowly accelerating backward as the bolt makes contact with the nut. As it's moving backward the spring force creates a reversed acceleration which will eventually overcome the threading forces. The nut carriage then accelerates toward the bolt carriage.

This model is not perfect as it works under many simplifying assumptions and does not truly grasp the lead screw feed rate, to bolt turning relationship. It provides a baseline understanding of system behavior that can be refined over time.

The rigid body dynamic simulation was used as in input for the transient structural analysis of the carriages. In Figure 14 we see where stress concentrations are forming. These results will need to be refined but show promising results. Under the current loading parameters a fully 3d printed design made of PLA can withstand the bolting process. The largest measured stress was 31.245 Pa well below 3.5GPa, which is PLA's yield strength.

© 2026 by CLIMBING CLANKERS

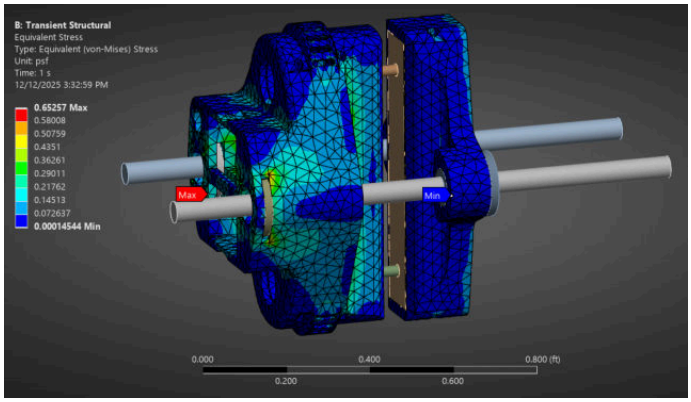


Figure 14: Transient Structural Analysis of Design

Through this transient structural analysis we limited the amount of structural aluminium made into the final model which both reduced weight and lowered cost.

3.3.2 Wheel Assembly

The wheel assembly consists of several distinct parts: a housing, compression spring, wheel mount, shaft, bearings, wheel, caps, pulley, and spacers (Figure 15). A total of four wheels will be used, with only the two lower wheels being driven.

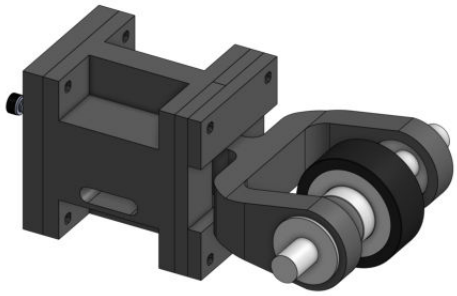


Figure 15: CAD Model of Wheel Assembly

The wheel rotates with the shaft using a set screw. One concern that was raised while designing the wheel was the possibility of the shaft moving or slipping out from the wheel axially. However, this was deemed to be a minimal issue as there would be no forces being applied in that direction. Any force that could be encountered would be much smaller than the force from the set screw pressing into the shaft and keeping it in place. During manufacturing, it was found that the shaft would slide axially due to the wheel moving in the extra space within the wheel mount. To address this, two spacers were designed and added to fill in the space and keep the wheel in place. This confirmed, however, that the shaft was positively retained by the set screw.

The two lower wheels that are to be actuated will also be connected to a pulley in order to be driven. The wheel mount bears against the compression spring, which is located within the housing (Figure 16). It is important to note that the wheel mount is free to slide axially in the housing, however caps are placed on the outside of the housing to prevent it from sliding out. Different clearances were tested between the mount and the housing to minimize material removal, eventually landing on a clearance of 0.01 in., which was imposed on all the parts within the housing.

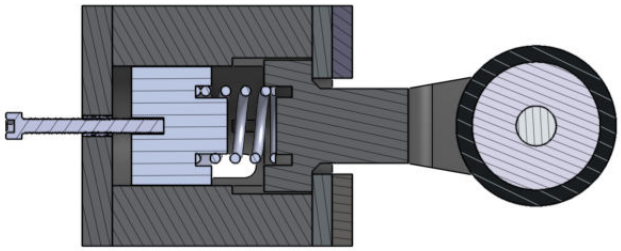


Figure 16: Cross-Sectional View of Wheel Assembly

The spring can be appropriately tensioned using a bolt, which is threaded into a heated insert that is bonded into the back part of the wheel assembly. As the bolt turns, it pushes against a 3D-printed part that compresses the spring, which results in a preload that acts as a baseline normal force pushing the wheel outward against the beam. By allowing the preload to be adjusted, the clamping force on the beam can be adjusted as necessary. The mechanism is demonstrated in the cartoon below (Figure 17).

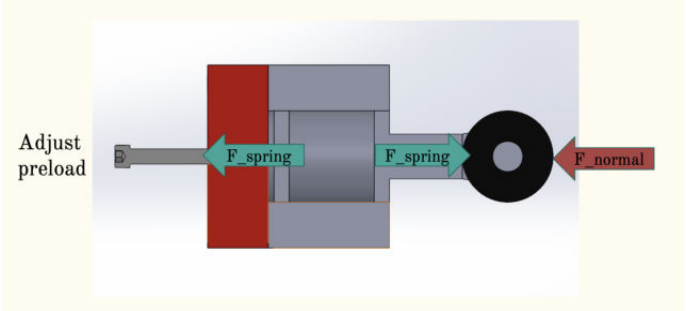


Figure 17: Spring Load Mechanism

As the spring changes in length, an opposing force is generated according to Hooke's Law (2).

$$F_s = kx \tag{2}$$

Where x is the displacement and k is the spring stiffness. By pre-compressing the spring, the wheel is given a nonzero, initial force to keep it pushed against the wall of the I-beam. This ensures that the wheel and wheel mount are not sliding into the housing due to the normal forces occurring when climbing. This results in the following relation for the spring force (i.e.

© 2026 by CLIMBING CLANKERS

force pushing against the wheel), where x_o is the initial displacement (3).

$$F_{s,final} = k(x_o + x) = F_n \quad (3)$$

This is equivalent to the normal force that the wheel will be experiencing from the beam. With the material coefficient of friction of rubber on aluminum to be estimated to be around 0.7 [15], and the weight of the robot to be assumed to be 50 lbs, the wheel is expected to experience around 35 lbs of normal force to support the robot's weight with a FOS of 2 (4).

$$F_n = \frac{FOS \cdot W}{n \cdot \mu_f} = \frac{2(50)}{4(0.7)} = 35.7\ lbs \quad (4)$$

Where n is the number of wheels. From this calculation, it is found that a spring stiffness of at least 63 lbs/in is necessary in order to have minimal displacement in the wheel while climbing (5).

$$k = \frac{F_n}{x_o + x} = \frac{35.7}{0.5 + 0.05} = 63.6\ lbs/in \quad (5)$$

This assumes that the spring is initially compressed 0.5 inches, and the wheel is only allowed to displace 0.05 inches.
The materials of the wheel assembly were chosen based on ease of manufacturing, cost, and availability. The housing components and wheel mount are all made of PLA, which allows them to be 3D-printed at the Makerspace. 1018 CD steel was chosen for the shaft of the wheel for its high yield strength in order to resist the stresses from the normal forces. The wheel is made out of a TPE rubber with steel bearings, as it was the most available choice.

A rudimentary hand calculation was performed on the heated insert to determine if the expected spring force is safe, as a concern was that the screw and insert would dislodge from the housing. The pull out resistance (i.e. the amount of force it would take to break the insert from the housing) was found to be greater than 405 lbs [16]. This is far greater than the expected spring force of 63 lbs, which means the insert would not dislodge.

A static structural analysis was run using an applied force of 35 lbs on the face of the wheel to simulate the conditions the wheel assembly will experience during operation. A maximum stress of 1450 psi was found, which was located on the shaft of the edge of the wheel mount (Figure 18). This result is compatible with the geometry, materials, and overall design of the wheel assembly as the stress experienced by the wheel mount is much lower than the yield strength of PLA, which is around 8000 psi [17]. That being said, to strengthen the part further, fillets were added at the stress points and the part was made thicker. Additional adjustments would be made during testing, if they were found to be necessary.

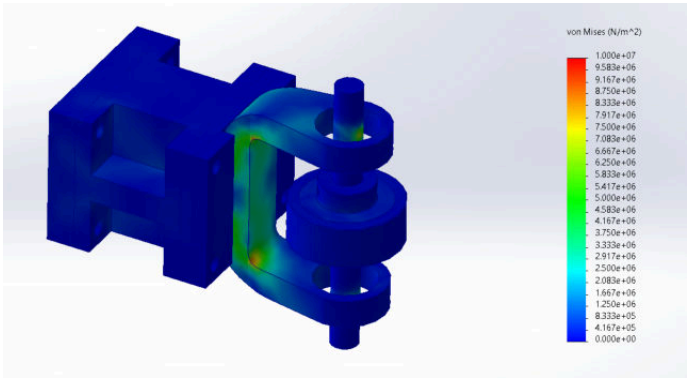


Figure 18: Stress Analysis of Wheel Assembly

In order to enable movement of the robot up the beam, the top two wheels will be driven by motors through a belt and pulley assembly. In this design, a pulley is directly attached to each active wheel (Figure 19) such that as the pulley is driven via a belt by the motor (Figure 20), the wheel turns as well. For now, the other attachments in the wheel are the same as for the free-spinning wheels. Once the wheel, pulley, and attachment method have been finalized, they will be modified as necessary to accommodate the pulley.

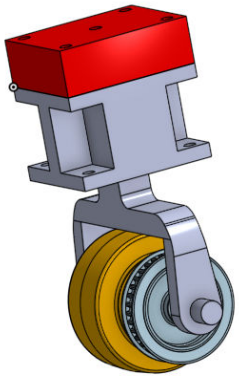


Figure 19: Wheel Module with Pulley Attached

© 2026 by CLIMBING CLANKERS

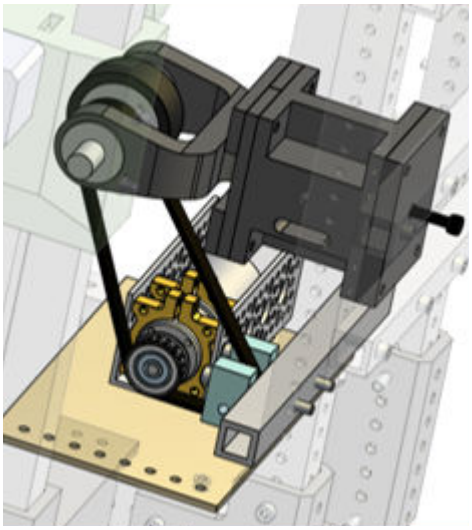


Figure 20: Belt and Pulley Assembly

The pulley and wheel selection heavily depend on each other, as the pulley must be able to be attached to the wheel assembly such that pulley rotation directly translates into rotation of the wheel on its shaft. In order to avoid permanent alterations of the wheel structure, it was determined that attachment by set screw to the wheel shaft would be ideal for the pulley on the wheel end. This cooperates with the selection of a wheel that adheres to the wheel shaft rotation due to its press-fit tolerance. Otherwise, pulley selection is entirely geometry dependent. The pulleys on the wheel end and motor end must have the same pitch tooth profile and pitch in order to be able to accommodate the same belt. As such, the belt itself must be compatible with the pulleys. Due to it being a complementary accessory to the chosen motor, an HTD timing pulley with a 5mm pitch was selected. Thus, an HTD timing belt was used and a compatible pulley was found for the wheel end of the assembly. Given that the bore of the motor pulley, and therefore related pulleys, was relatively small, at a diameter of 6mm, and the wheel shaft diameter was 0.5 in, there was limited availability of compatible pulleys. As such, one was selected which had the correct tooth profile and pitch, but a different width from the belt and the motor pulley. Such a discrepancy is not as consequential, though still suboptimal. Otherwise, function of the belt and pulley assembly proceeds as intended.

The pulley itself is a purchased metal pulley. While this will increase costs as compared to 3D printing a custom-designed pulley, it is necessary because a 3D printed pulley will not be able to handle the load applied to it by the motor, especially not over many cycles.

The motor has been selected based on the locomotion requirements. A DC motor is used for high torque capabilities, as well as its compatibility with planetary gearboxes that can output even more torque at high ratios while being compact. The motor and planetary gearbox are selected based on the weight of the robot, which was assumed to be 50 lb. – or 222.4 N – at the time of motor selection. The radius of the wheels are 1 in., or 0.0254 m. As such, the total required torque is

$$T = Fr = (222.4\ N)(0.0254\ m) = 5.649\ N*m \quad (6)$$

Two wheels are carrying this load, so each wheel carries 2.825 N*m. Using this rough estimate and to aim for a factor of safety of at least greater than 2, a gear ratio of 50:1 was initially chosen for the planetary gearbox. A higher ratio was then used for further factor of safety concerns. The output torque is the torque of the motor multiplied by the gear ratio. A geared motor – that is, a motor which arrives with a planetary gearbox already installed – has been chosen for reduced size and ease of assembly. It produces an output torque of 15N*m with a gearbox ratio of 189:1. That means that in regards to climbing ability, each wheel will have a factor of safety of

$$\frac{15N*m}{2.825N*m} = 5.3 \quad (7)$$

In order to reduce considerations and potential complications during the prototyping stage, these are approximately the torque and factor of safety across the entire assembly as the pulleys on the motor and wheel ends do not have significantly different diameters, so there are no major additional gear ratios.

3.3.3 Frame

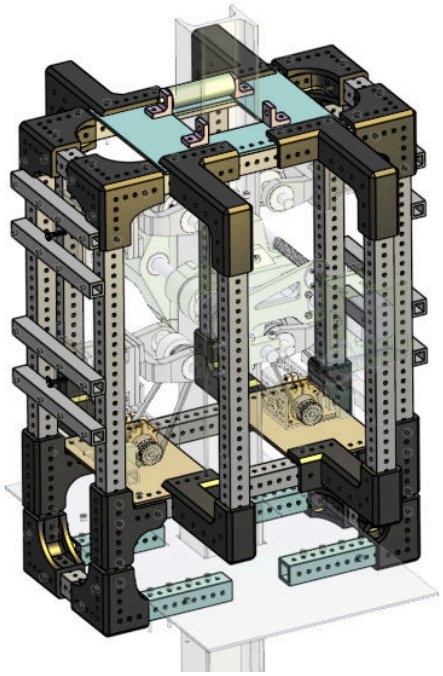


Figure 21: Frame Assembly

The frame is designed to support the weight of the locomotion system, fastening system, electrical system, and attachment components, while allowing for smooth movement of the robot

© 2026 by CLIMBING CLANKERS

up and down the beam. The overall dimensions, only considering the structural channels, are 14 in. x 22.5 in. x 7.5 in. or 0.36 m. x 0.57 m. x 0.19 m. which approximately fulfills the target specification of 0.5 m. x 0.5 m. 0.5 m. with a slight extension in height. For portability and weight reduction, the frame dimensions have been made as small as possible while maintaining sufficient space to install and remove components at will, as well as provide reasonable flexibility on installation locations in order to fulfill the objective of modularity.

The material selection for the structural members of the frame heavily considered cost efficiency, weight, and strength. Based on these factors, aluminum alloy square tubing was chosen, due to Aluminum 6061-T6 being one of the most commonly used materials in manufacturing thus easily accessible. Pre-drilled square tube extrusions have been chosen as the holes across and along all four faces as well as the pitch being compatible with both M5 and 10-32 fasteners allowed for general fastener consolidation as well as the aforementioned modularity in sub-assembly attachment to the frame.

Along with the foundational structural members, the frame also consists of smaller aluminum channels which have been outsourced; they are used to attach the wheel modules to the frame and run across the width of the prototype. The bottommost members are 3D printed as opposed to purchased for the purpose of cost reduction. As they are used for mounting of electrical components, they will not experience major load-bearing. Pre-drilled tubes run externally along the vertical axis in order to support the fastening assembly. Besides the frame structure itself, custom corner gussets have been designed to attach the channels together such that stability and rigidity is maximized. Custom attachment accessories have also been designed to accommodate the fastening assembly mounting channels. Otherwise, a 3D printed roller mechanism has also been designed in order to guide alignment of the I-beam in directions not supported by the wheel modules.

Including its own weight, the frame must be able to withstand the weight of all of the systems and the force exerted on it by the wheel spring system without deformation or failure. In order to verify this, a static structural analysis of the frame with the locomotion system integrated has been conducted. As it has not yet been integrated, the fastening system is considered in this study as a load with an assumed value of 20 lbf. It is assumed that the force exerted by the wheels on the beam is sufficient to keep the robot stationary on the beam without falling and that a predetermined value of 31.25lbf needed for the wheels to do this is exerted back on the frame by the wheel assemblies. Standard earth gravity is used to implement the weight of the robot.

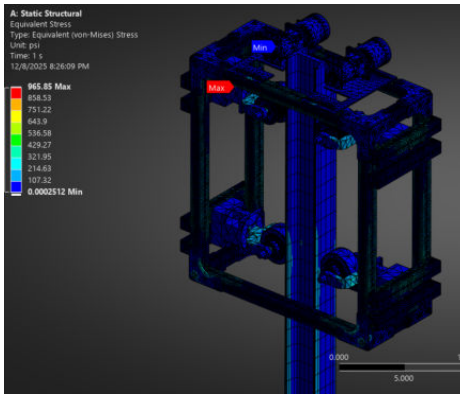


Figure 22: Frame Static Structural Analysis Stress

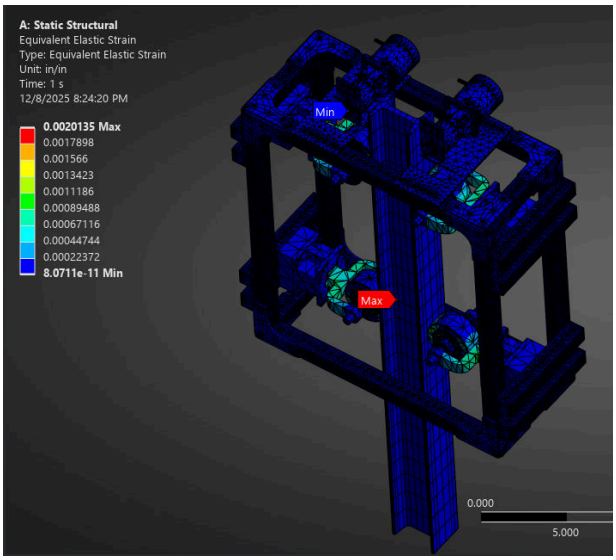


Figure 23: Frame Static Structural Analysis Strain

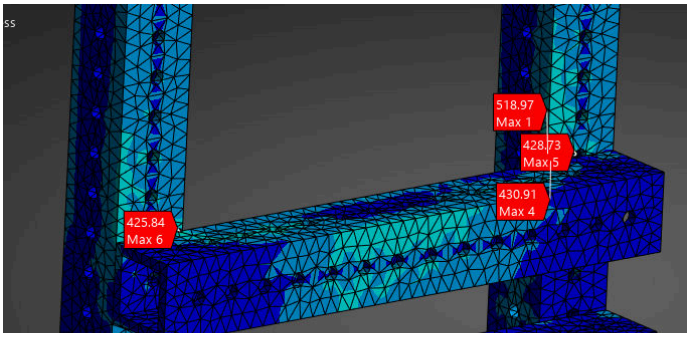


Figure 24: Frame Static Structural Analysis Local Max Stresses

Based on the simulation, the frame experiences relatively little equivalent stress (Figure 22) and essentially negligible equivalent elastic strain (Figure 23). Using a yield strength of 40,000 psi for Aluminum 6010-T6 [17] a factor of safety ranging from 70 to over 100, based on the local maximum stresses (Figure 24) on the frame, is obtained.

© 2026 by CLIMBING CLANKERS

These results neglect to consider the real load created by the integration of the fastening assembly, nor the torques generated by the active systems or the additional weight from electrical components. Additionally, in practical applications the loads are not static and will constantly change. However, due to the factor of safety being significantly higher than expected, it can be reasonably assumed that the frame configuration is more than sufficient even if these factors are considered. That is to say, there are no significant issues with the chosen frame materials, geometry, or attachments, and the frame is not expected to be at risk in any capacity. In order to further verify in the future, a transient structural analysis can be conducted to obtain more precise readings.

3.3.4 Energy and System Control

To estimate the power supply required for the robotic system, a conservative estimation for the power requirement was developed and summarized in Table 8.

Table 8: Power Estimation of Robot Electronics

Subsystem	Quantity	Rail (V)	Total Current (A)	Power (W)
Climbing Motor (Brushed DC)	2	12	20	480
Bolting Motor	2	12	16.7	401
Clamping Motor	1	24	1.25	30
Miscellaneous (Sensors, controller, driver)	N/A	5V	N/A	~10

The robot operates in two primary modes: climbing and bolting. Therefore, the total power and operating current for each mode can be estimated by summing the relevant subsystem power demand based on Table 8 and dividing by the bus voltage. The mode-based power and current estimates are summarized in Table 9.

Table 9: Power Estimation of Robot Electronics

Bus Voltage: 24V	Total Power (W)	Peak Operating Current (A)
Climbing Mode	490	20.4
Bolting Mode	441	18.4

The worst-case operating current occurs during climbing and is approximately 20.4A. To account for startup and stall spikes, a safety factor of 2 was applied to estimate peak currents (8):

$$I_{peak} = 2 * 20.4 = 40.8A\ (\approx 40\ A) \quad (8)$$

This indicates the power system should be capable of supporting about 40A peak current. However, for the current prototype, the system is not powered by an onboard battery. Instead, a wired external AC-to-DC power supply is used. This decision was made because the prototype is mainly intended for controlled testing and demonstration, where continuous runtime and portability are less important than stable power delivery, ease of troubleshooting, and safety.

The selected power supply is a 24 V, 41.6 A, 1000 W AC-to-DC switching power supply. Since the robot is powered through a wired supply, the previous battery capacity estimate is not used as a design requirement for the prototype. Instead, the main requirement is that the supply can provide sufficient continuous power for the expected operating modes while the wiring, fuses, and motor drivers tolerate short transient loads. Although the estimated peak current is approximately 40 A, this value represents a conservative transient case rather than the expected continuous operating current. The nominal climbing current is closer to 20.4 A, which is within the continuous capability of the 24 V, 41.6 A power supply.

For a future battery-powered version, the average power should be estimated based on the amount of time the robot spends in each operating mode. Assuming a 10-minute demonstration with approximately equal time spent climbing and bolting, the average power of 466 W is calculated from the climbing power of 490 W and the bolting power of 441 W:

$$Wh = Pt = 466 * \frac{10}{60} = 77.7\ Wh \quad (9)$$

Converting to amp-hour to compute the charge capacity for the power supply (10)

$$Ah = \frac{Wh}{V} = \frac{77.7}{24} = 3.24\ Ah \quad (10)$$

After accounting for power losses, battery inefficiency, and the fact that a battery should not be fully discharged, a 5–6 Ah battery would be a reasonable minimum estimate for a future onboard battery version. However, for the current prototype, a wired 24 V, 41.6 A, 1000 W AC-to-DC power supply is used instead, so battery capacity is not a direct design requirement for the final prototype.

Using the Arduino IDE to program the software, the Arduino Mega acts as the main controller for the robot. It receives input signals from the limit switches, photoelectric sensor, ultrasonic sensor, encoder, and current sensors. Based on these sensor inputs, the Arduino controls the motor drivers for climbing, bolting, and stepper-driven plate feeding. The control system follows a state-based sequence: the robot begins in a wait state, climbs upward when started, detects the target hole using the photoelectric sensor, holds position during fastening, feeds the bolting mechanism forward, tightens the bolts using motor current feedback, retracts the fastening mechanism, and then descends after the fastening cycle is complete.

© 2026 by CLIMBING CLANKERS

The wiring diagram shows the relationship between the power and control systems. High-current 12V motor power is routed separately from the low 5V signal wiring, while all control signals are referenced to a common ground. The limit switches provide digital feedback for motion boundaries, the current sensors monitor bolting motor load, and the photoelectric sensor provides alignment feedback. This layout allows the robot to operate through a controlled sequence while also providing manual stopping and return behavior during testing (Figure 25).

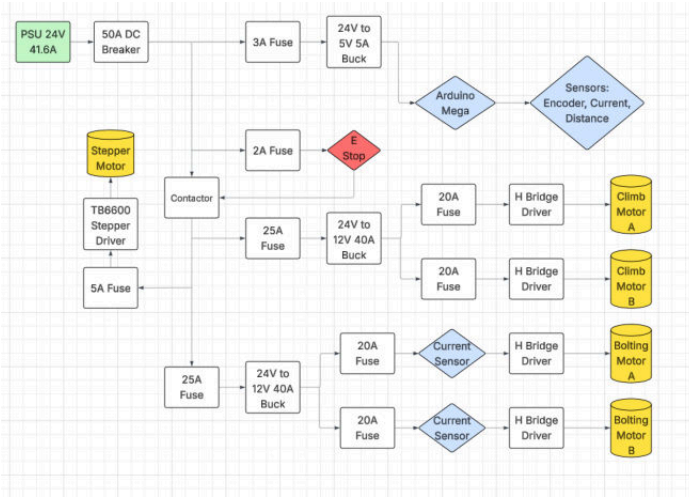


Figure 25. Electronic Power Distribution

The external 24 V, 41.6 A power supply provides the main power source for the prototype. This wired setup was selected for reliable bench testing and demonstration, reducing the need for onboard battery management during the current design stage.

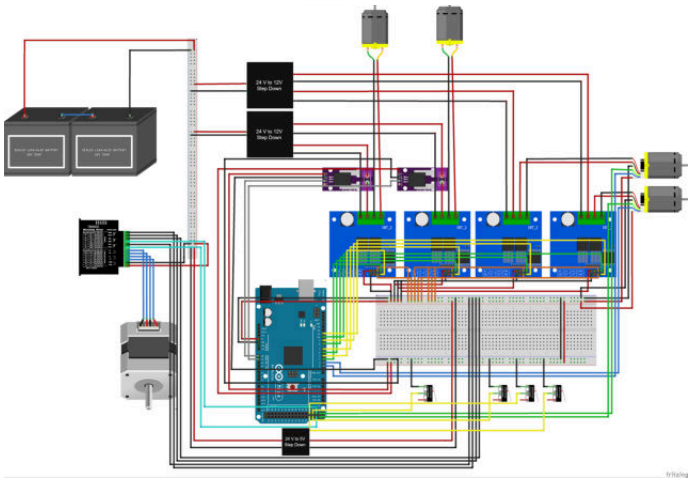


Figure 26. System Wiring Diagram

The wiring diagram shows the integration of the Arduino Mega, motor drivers, DC-DC converters, sensors, and limit switches. The 24 V power bus supplies the main motor loads, while buck converters step the voltage down for the 12 V motor subsystems and 5 V control electronics. The Arduino Mega acts as the main controller and uses sensor feedback to coordinate the full operating sequence, including climbing, alignment, fastening, and retraction (Figure 26).

For the climbing system, the encoder motor provides speed feedback so the Arduino can regulate the climbing motor to a commanded speed using PI control instead of simply running it at a fixed PWM value. This allows the robot to climb more consistently even when the load or friction changes. The photoelectric sensor is used for alignment by detecting when the robot reaches the target hole location on the beam. Once the fastening position is reached, the bolting motors are controlled using current sensors. Since motor current increases as tightening resistance increases, the current sensors provide a rough torque-control method for detecting when the bolts have reached the desired tightening condition. The limit switches are used to define motion boundaries for the feeding and retraction mechanism, such as detecting when the bolt carriage has fully moved forward or returned backward. They also provide safety feedback so the robot can stop or reverse motion when a mechanical limit is reached. Overall, the wiring and control system allow the robot to operate as a feedback-based sequence rather than a purely open-loop mechanism.

3.4 Design For Sustainability

When designing the robot, there were several factors to consider in order to create a product that would be sustainable for the environment and the community. An impact matrix was created to determine the possible ways the robot might be negative for sustainability (Table 10).

© 2026 by CLIMBING CLANKERS

Table 10: Impact Matrix

	Raw Materials	Suppliers	Production	Distribution	Use	EOL
Material Use	Aluminum, steel, PLA	Packaging, spare parts	Machining, 3D printing	N/A	2–4 month lifespan	Metal, e-waste recycling
Energy Consumption	Metal extraction energy	Factory electricity use	CNC, printing, testing	Transport fuel	Motor and sensor power	Recycling, disassembly energy
Solid Waste	Metal scrap	Packaging and machining waste	Fabrication waste	None	None	Expended components
Toxic Emissions	Extraction emissions	Factory emissions	Printing fumes, lab emissions	Transport emissions	Heat output	Component degradation
Human Resources	Standardized safe materials	Skilled manufacturing labor	Student and technical labor	Trained deployment staff	Reduced worker exposure	Technician-led refurbishment
Local Economic Development	Imported materials	Specialized vendors	Automation reducing manual labor	Transportation infrastructure	Workers replaced	More recycling facilities
Cost	High	High	High	Low	High maintenance	Low
Environmental Impact	Excess material	Unsustainable sourcing	Waste and power use	Transport emissions	High energy demand	Reuse and recycling

The impacts on energy consumption and material use were prioritized in the development of this robot, given that this is a prototype that should be easy to build and test without requiring substantive resources that are inaccessible by the local community. The robot would undoubtedly require aluminum, steel and PLA materials for production, due to the various functions of the robot requiring different material properties. As such, these needed to be minimized as much as possible, which would also help drive down production costs.

3.4.1 Design Strategy

To address this, the selected design strategy was to use 3D-printed PLA components where possible, while using aluminum and steel only in parts that may experience high amounts of stress, vibration, and/or load cycling. While PLA plastic is bad for the environment, it enables rapid prototyping and low-waste fabrication through additive manufacturing, reducing excess material removal associated with subtractive processes such as machining. As long as the parts were toleranced correctly, the exact amount of PLA needed would be used each time. On the other hand, steel and aluminum would need to be machined, and the excess material would be wasted. Standardized and modular components were also incorporated to reduce unnecessary material usage and simplify replacement of damaged parts rather than full-system replacement.

By prioritizing the use of PLA, the required energy consumption was also reduced for non-critical components. PLA-based additive manufacturing generally requires lower processing temperatures and less machining energy compared to many metal fabrication methods. Using lightweight PLA material also reduced the overall system mass, lowering motor power requirements during operation.

3.4.2 Brainstorming Results

Several ideas were developed to optimize the amount of material used and decrease the amount of aluminum/steel parts, as well as reduce energy consumption:

- Design geometry to reduce excess material
- Replace non-critical metal parts with 3D-printed parts
- Standardize fasteners to avoid over-purchasing
- Reduce print failures through tolerance optimization
- Modular design for reuse and repair
- Minimize number of unique parts
- Use passive mechanisms (springs, magnets) instead of powered systems

3.4.3 Implementation

A key implementation of this strategy was switching from aluminum gussets to 3D-printed components for the frame. The design of the gussets were optimized such that they could still provide the necessary strength for the frame while being made out of PLA. This removed the need to machine multiple parts out of aluminum through time- and energy-intensive processes such as water jetting.

Additionally, a novel self-threading mechanism was designed and applied in multiple 3D-printed components. As the screw is inserted, its threads plastically deform and cut into the surrounding material, creating a secure mechanical engagement without requiring separate threaded inserts, tapped holes, or extra nuts.

Lastly, several passive mechanisms were incorporated in the robot. The plate was retained in the fastening system through magnets, which reduced the energy consumption during operation as the alternative would possibly require extra motors. The wheels also provided a clamping force on the beam using a spring-loaded design, without any additional active mechanisms. In fact, the robot was able to hold onto the beam with low to none holding torque.

4. FABRICATION & ASSEMBLY

The completed assembly of the climbing robot for I sectioned column assembly is attached below (Figure 27)

© 2026 by CLIMBING CLANKERS

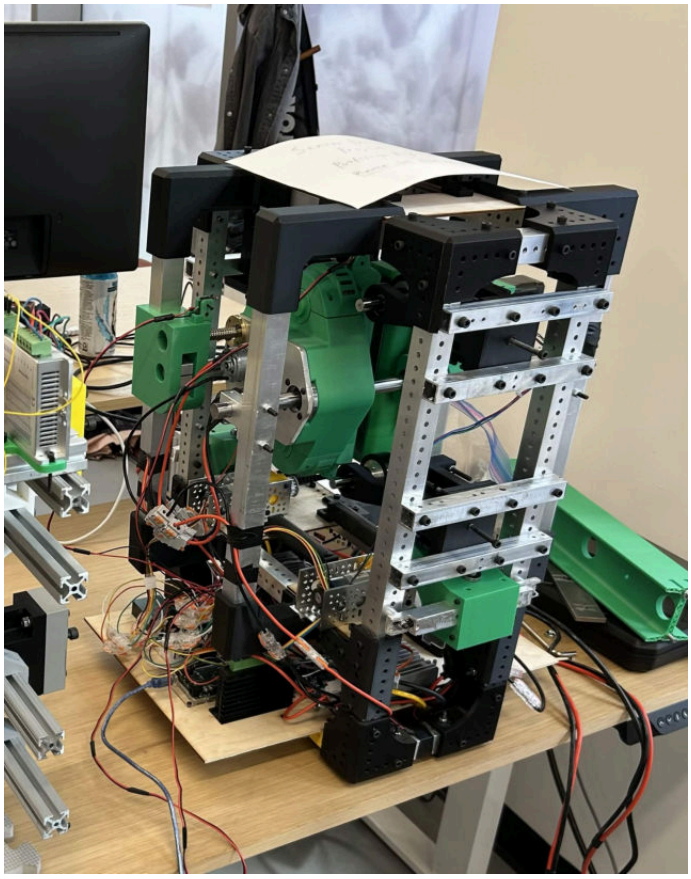


Figure 27: Complete Assembly of The Climbing Robot

4.1 Fabrication

The robot was fabricated using a combination of custom-made parts and off-the-shelf components. The overall structure was designed to be modular so that the climbing mechanism, fastening mechanism, electronics, and frame could be assembled and tested separately before being integrated into the final prototype. This approach was useful because several parts required redesign after initial testing, especially the wheel mounting system, belt tensioning system, and fastening carriage.

Several components were fabricated in-house. The main frame was built from aluminum tubing, which was cut to length using a circular saw and assembled with fasteners. This provided a lightweight but rigid structure for supporting the climbing motors, fastening assembly, and electronics plate (Figure 28).



Figure 28. Segmented Aluminium Channels

Some flat mounting components, such as motor mounting plates, and the electronics support plate, were laser cut from birch wood for rapid prototyping. These plates allowed the motor and electronics layout to be tested and adjusted with a hand drill before committing to a full assembly.

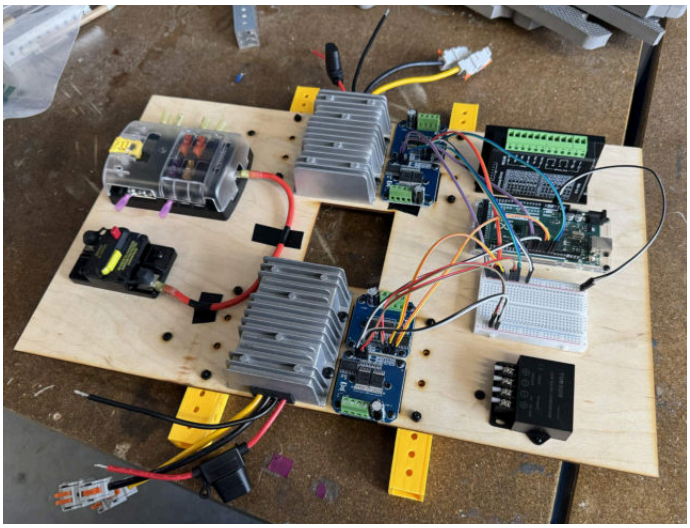


Figure 29: Mounted Electronics Onto Laser Cut Birch Wood

A large portion of the prototype was made using PLA 3D printing. The 3D printed components included the wheel housings, mounting brackets, sensor holders, belt tensioner supports, and several fastening assembly parts. 3D printing was useful for the prototype because it allowed complex shapes to be produced quickly and modified between design iterations. For example, several mounting brackets were redesigned to improve clearance, increase stiffness, or better align with the purchased motors and shafts. Printing orientation was heavily considered during the fabrication process because the mechanical strength of FDM-printed parts is anisotropic. For

© 2026 by CLIMBING CLANKERS

example, the 3D-printed brackets were printed diagonally in a standing orientation to improve their ability to withstand loads from multiple directions. Other printed components were also oriented carefully to ensure that layer adhesion would not become the limiting factor in the part's strength.

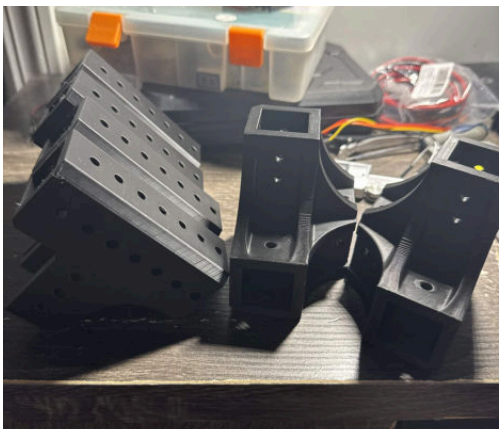


Figure 30: 3D Printed Frame Connector

The fastening mechanism also used custom printed parts to hold and guide the bolt/nut carriage during forward feeding and retraction. Some higher-load components were fabricated from aluminum plates using waterjet cutting. These included the bolt carriage and nut carriage components in the fastening assembly. Aluminum was selected for these parts because they experience higher contact forces and alignment loads during the fastening process. During the fabrication process alignment of the nut and bolt carriage and much of their construction was done in conjunction with the frame and electronics on a supportive rig which allowed for validation of the linear actuation, suspension, and dual lead screw alignment before full assembly.

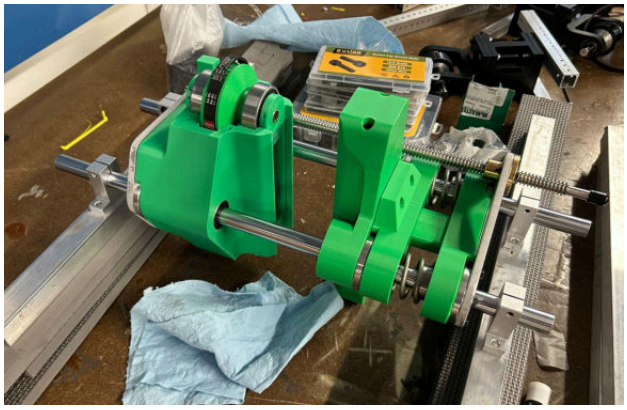


Figure 31: Fastening Rig With Dual Leadscrew Validation

The remaining components were purchased off the shelf. These included the DC gear motors, motor drivers, bearings, shafts, springs, timing belts, pulleys, fasteners, limit switches, photoelectric sensor, ultrasonic sensor, encoders, current sensors, and power electronics. For the prototype, an external wired 24 V AC-to-DC power supply was used instead of an onboard battery. This allowed the robot to be tested with a stable power source during development and reduced the need to package a battery system on the robot during the demonstration stage.

4.1.1 Challenges Encountered

Several manufacturing and assembly challenges were encountered during fabrication. One major challenge was tolerance mismatch between 3D printed parts, laser-cut plates, and purchased components. Some printed holes and slots required sanding, drilling, or redesigning to fit shafts, bearings, and fasteners properly. These processes took a majority of the time during assembly.

The belt drive also required repeated adjustment because belt tension, pulley alignment, and wrap angle strongly affected climbing performance. In the early prototype, the tensioner increased belt tension but did not provide enough belt engagement around the driving pulley. This reduced the effective wrap angle, meaning fewer belt teeth were engaged at once. During climbing, belts would loosen slightly, causing tooth skipping. The belt path and tensioning method were adjusted to increase wrap angle, improve tooth engagement, and maintain more even tension on both belt spans.

Another issue was found in the wheel module where the clamping load from the spring created high contact pressure on the back of the 3D printed wheel housing. Since the adjustment bolt was steel and the housing was PLA, repeated tightening and motion potentially caused the bolt to dig into or wear down the printed surface. This also made the clamping force less consistent over time. To solve this, a thin aluminum block was inserted at the back of the wheel module as a reinforcement plate. The aluminum insert spreads the load over a larger area, prevents direct steel-on-PLA contact, and improves the durability of the clamping mechanism while still allowing the main housing to remain 3D printed for prototyping (Figure 32).

© 2026 by CLIMBING CLANKERS

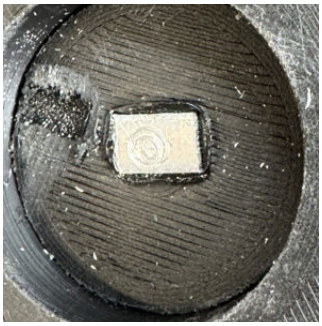


Figure 32: Bandsaw Aluminium Block Heated Inserted Onto Wheel Module

Integration of the mechanical and electrical systems into the same robot frame. The wiring, power supply leads, motor drivers, sensors, and Arduino Mega had to be arranged so that they did not interfere with the climbing wheels, belt path, or fastening motion. The final wiring layout separated high-current motor wiring from low-voltage sensor and control wiring as much as possible. The 24 V supply was distributed to the motor drivers and buck converters, while the Arduino and sensors used the lower-voltage control rail. Limit switches, current sensors, and the photoelectric sensor were mounted so that they could provide feedback to the control system during climbing, alignment, fastening, and retraction.

These challenges were addressed through iterative prototyping and modular assembly. Parts were first tested individually, then assembled into subsystems, and finally integrated into the full robot. The use of 3D printing, laser cutting, and simple machined aluminum parts made it possible to quickly revise the design when clearance, alignment, or stiffness issues were found.

If this design were converted into a series product, several manufacturing processes would change. The PLA 3D printed parts would likely be replaced by injection-molded plastic, machined aluminum, or cast components depending on the required strength and production quantity. Laser-cut birch prototype plates would be replaced with aluminum or steel sheet-metal parts made using CNC cutting, bending, and fixture-based assembly. Manually cut aluminum frame members would be replaced with CNC-cut extrusions or welded/bolted production frames with controlled tolerances. Assembly would also use dedicated jigs and fixtures to improve alignment of the wheels, belts, shafts, and fastening carriage.

Other mechanisms would also be adjusted in a future design iteration. Instead of using a belt-driven climbing system, a worm drive would be a strong alternative because it provides a large gear reduction and has minimal back-driving. This would help the robot hold its vertical position more securely without relying only on the internal gear ratio of the motors. In the current prototype, the robot mainly depends on motor gearing and holding torque to resist slipping when stopped, which can still require power or create loading on the drivetrain. Adding an active braking mechanism would further improve safety and reduce power consumption by mechanically locking the climbing system when the robot needs to hold position. These changes would make the climbing system more reliable, energy efficient, and better suited for a production version of the robot.

The electronics would also be redesigned for production. Instead of using separate motor drivers, buck converters, jumper wires, and prototype wiring, the final product would likely use a custom PCB. Connectors, strain relief, fuse protection, and cable routing would be standardized to improve reliability and resilience against vibration. Additionally, rather than a walled AC to DC power supply, a battery would be used for the final assembly.

4.2 COST ANALYSIS

The total cost of the prototype is categorized across the electrical system, frame, fastening assembly, wheel assembly, pulley assembly, and standardized fasteners.

Table 11: Cost Summary

Sub Assembly	Cost
Electronics	387.86
Frame	193.92
Fastening	372.63
Wheel	169.27
Pulley	217.12
Fasteners	55.93
Total	$1,396.73

The highest cost comes from the electronics due to the large number of components required to support all of the active systems with adequate power, as well as provide safety measures in case of unexpected system failures. Otherwise, the most expensive components were the motors; this can be seen in the fastening and pulley systems carrying the highest costs aside from the electronics. Given that the usage of motors in these sub-systems is nonnegotiable, cost reduction strategies must focus on compensation elsewhere in the prototype, as outlined below. Additionally, if the cost of actuators becomes a major concern in mass production, a reduction of motors in favor of mechanical transmission systems; however, this may in turn require extra purchases to construct such mechanisms.

© 2026 by CLIMBING CLANKERS

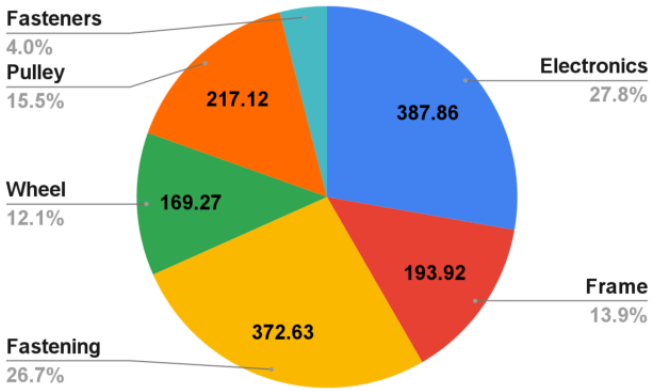


Figure 33: Cost Chart

Ultimately, the project cost $1,396.73, which was about $400 over the typical $1,000 senior design budget. However, after discussion and negotiation, the additional cost was supported through extra funding from the senior design class and the project mentor. This allowed the team to complete the build, integrate the full system, and successfully demonstrate the robot during the senior design showcase.

4.2.1 Cost Reduction Strategy

Several strategies were used to reduce the overall project cost. (1) Components were 3D printed whenever possible instead of being purchased as raw metal stock and machined, which helped reduce both material and manufacturing costs. (2) Fasteners were also reused across assemblies when appropriate, and isolated components were outsourced when purchasing materials in bulk would have been more expensive. (3) Design relied on standardized components wherever possible and was simplified to reduce the total part count. Together, these decisions helped control the budget while still allowing the robot to be fully built and tested.

4.2.2 Series Production Cost Impact

If the system were produced at scale, the overall cost per unit would likely decrease substantially. (1) Bulk purchasing would reduce individual component costs. (2) Manufacturing costs per unit would decrease due to economies of scale. (3) Labor costs would decrease through increased automation. (4) Tooling costs, such as molds and fixtures, would increase initially but reduce the long-term cost per unit. (5) Overall, the system cost would become significantly lower in large-scale production.

5. TESTING & EVALUATION

The proposed solutions will be evaluated as distinct entities in order to ensure full functionality of each assembly before complete integration of the top level assembly. The fastening assembly will be tested to successfully locate the beam holes and align the plate correspondingly. Next, it should insert and rotate two bolts into the plate/beam holes. The wheel assembly will commence testing with the motor, belt, and pulley sub-assembly. Once the functionality of the driven wheel system has been verified, the overall locomotion function will be tested in its ability to traverse up the I-beam without significant slippage or resistance.

Following successful evaluations of individual assemblies, they will be integrated progressively and have their combined functions tested in sequence until the top level assembly is completed. This assembly will be assessed in its ability to complete all aforementioned functions while maintaining frame stability. All testing, especially final evaluations, will be conducted multiple times in order to ensure repeatability and reliability of results.

Table 12: Test Plan

No.	Test	Location	Schedule	Data
1	Climb I-beam	CREO	After locomotion assembly	Distance/time
2	Align tool to hole	CREO	After sensor integration	Position error
3	Fasten bolt	CREO	After fastening assembly	Timestamp logs
4	Tighten bolt	CREO	Fastening test	Current + torque check
5	Climb with plate loaded	CREO	Subsystem integration	Video/inspection
6	Operate full robot	CREO	Prototype testing	Visual/deflection
7	Monitor during operation	CREO	Electrical integration	Multimeter values
8	Run multiple cycles	CREO	Final integration	Fault/reset notes
9	Full system test	CREO	Final testing	Video + time

The system was evaluated based on key performance parameters:

Table 13: Test Parameters

No	Parameter	Threshold
1	Climbing Speed	≥ 0.10 m/s
2	Alignment Accuracy	±2 mm
3	Bolt Cycle Time	≤ 15 s
4	Torque	8–12 Nm
5	Plate Retention	No slip
6	Structural Integrity	No deformation

© 2026 by CLIMBING CLANKERS

7	Power Stability	~24 V maintained
8	Electrical Reliability	No failures
9	Full Task Completion	Successful operation

Testing was conducted at the NYU Center for Robotics and Embodied Intelligence Lab (CREO) using a controlled I-beam test setup, as shown in Figure X. The setup consisted of an aluminum I-beam with two M6 tapped holes drilled through its cross-section. These holes allowed the vertical 3D-printed I-beam fixture to be inserted and secured using M6 studs, creating a stable test structure for evaluating the robot's climbing, holding, alignment, and fastening performance. (Figure X).



Figure 34: Test Setup

5.1.1 Test and Evaluation Results

The following parameters represent preliminary testing results. Due to schedule constraints, some parameters were not fully tested in time and therefore require further refinement with additional software integration and extended testing.

Table 14: Test Result

No	Parameter	Threshold
1	Climbing Speed	4.2 cm/s
2	Alignment Accuracy	N/A
3	Bolt Cycle Time	85 seconds
4	Torque	N/A
5	Plate Retention	No slip
6	Structural Integrity	No deformation
7	Power Stability	~24 V maintained
8	Electrical Reliability	No failures
9	Full Task Completion	Successful operation

Based on the preliminary results, the robot was able to complete the full task sequence successfully, including climbing, holding position, and completing the fastening operation. The measured climbing speed was 4.2 cm/s, which is lower than the original speed requirement. However, this result does not represent the maximum capability of the locomotion system, since the robot was only operated at approximately half of its available PWM signal, around 115 out of 255. A lower speed was intentionally used during testing to reduce belt wear and minimize the risk of belt skipping during repeated trials. Therefore, the target climbing speed could potentially be reached with further tuning and operation at a higher PWM value.

Alignment accuracy was not measured as a specific numerical value because the automated alignment mechanism was still being refined. During testing, the wheel system produced sufficient normal force to hold the robot on the I-beam, but minor slipping due to the artificial PLA I beam surface affected precise positioning. To address this, a homing and alignment mechanism was added so the robot could better locate and settle at the fastening position before starting the bolting sequence. Similarly, torque was not measured as an exact value because the fastening system was operated using an open-loop timing approach. Once the plate was seated against the I-beam, the fastening motors were run for a fixed 20-second duration instead of closing the loop based on measured torque.

At the time of the report six full test runs were completed using the final test setup. Out of these runs, four successfully achieved nut engagement with the bolt threads, allowing the plate to be secured to the I-beam.

6. CONCLUSION & FUTURE WORK

This project addressed a safety and efficiency challenge in steel construction by developing a climbing robot capable of traveling along a vertical I-beam and performing a bolted plate-fastening operation. Through requirement definition, concept selection, analytical calculations, prototyping, and system testing, the team developed a functional robot consisting of a wheel-based locomotion system, fastening assembly, structural frame, and integrated electronics platform. The final prototype successfully demonstrated the main intended operation during the senior design showcase, including climbing, holding position, and completing the plate-fastening sequence.

The design met several of the major project specifications. The robot was able to remain attached to the I-beam without plate slip, maintain structural integrity without visible frame deformation, and operate without major electrical failures.

© 2026 by CLIMBING CLANKERS

Power supply stability was also maintained at approximately 24 V during testing. The full task sequence was successfully completed, and four out of six full test runs resulted in the nut latching onto the bolt threads and securing the plate. These results demonstrated that the selected system architecture was feasible and that the robot could perform the core climbing and fastening functions.

Some specifications were only partially met or were not fully quantified due to testing and schedule constraints. The measured climbing speed was below the original target; however, the robot was intentionally operated at a reduced PWM value of approximately 115 out of 255 to reduce belt wear and improve reliability during repeated testing. This suggests that the locomotion system may be capable of higher speeds with additional tuning. Alignment accuracy was not measured numerically because the automated homing and alignment mechanism was still being refined to address minor slipping during positioning. Similarly, fastening torque was not measured as a specific value because the final fastening sequence used an open-loop timing method rather than a closed-loop torque-controlled process.

The cost analysis showed that the project exceeded the original senior design budget, with the largest cost categories coming from the total system components, electronics, fastening assembly, wheel/pulley components, frame, and fasteners. However, with additional support of $200 from the senior design class and $200 from the project mentor, the robot was successfully built, tested, and delivered. Overall, the final prototype validated the main design concept and demonstrated a successful proof-of-concept for an I-beam climbing and fastening robot.

6.1 Future Work

Future work should first focus on improving the belt tensioning and pulley system. Due to schedule constraints, the final belt tensioning setup was functional but not fully optimized. During testing, the belt occasionally slipped off the bearing, which affected drivetrain reliability. A more robust timing belt pulley or guided tensioning mechanism should be designed to improve belt tracking, reduce wear, and provide more consistent climbing performance.

Additional testing should also be conducted on the fastening system. The current prototype used an open-loop timed bolting sequence, but future tests should collect more data on motor current rise during tightening. This would allow the fastening process to be improved into a current-tracking or feedback-based control system instead of relying only on a fixed run time. Continued testing would also help shorten the cycle time, improve alignment repeatability, increase the factor of safety, and compile more conclusive performance results.

Beyond improving the current prototype, the design could be expanded to support horizontal traversal and a more practical setup procedure for real construction applications. Most importantly, this senior design project provides a strong foundation for continued research. The team plans to continue testing and refining the robot with the project mentor, with the goal of further developing the system and potentially preparing a co-authored paper based on the robot design, testing results, and future improvements.

ACKNOWLEDGEMENTS

The project team would like to express sincere appreciation to Professor Ludovic Dominique Righetti, the project mentor, for his invaluable guidance, technical expertise, and continuous feedback throughout the design process. His insights into robotics, autonomous systems, and overall project direction were fundamental in shaping the team's technical approach. The team would also like to thank Professor Debra Laefer for providing the I-beam used for testing and for sharing her knowledge of I-beam structures, which helped the team better understand the real-world application and scope of the project. Additionally, the team would like to thank Leon Seetoo for providing helpful insights during the assembly and testing phases of the robot. His suggestions and feedback helped the team troubleshoot issues, improve the setup, and refine the robot's performance during validation.

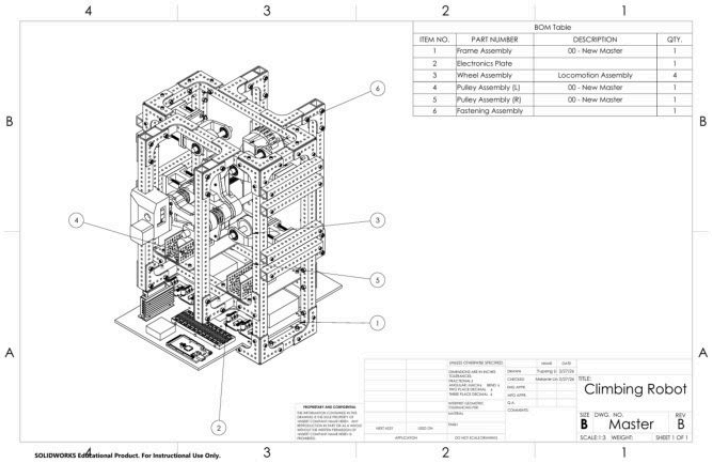
REFERENCES

[1] Bureau of Labor Statistics. (2023). *Census of Fatal Occupational Injuries*. U.S. Department of Labor.
[2] American Institute of Steel Construction (AISC). (2016). *Specification for Structural Steel Buildings (ANSI/AISC 360-16)*.
[3] A. M. Sadegh and J. Xiao, "Modular wall climbing robot with transition capability," U.S. Patent 7,520,356, Apr. 21, 2009.
[4] J. Liu, J. Smith, and R. Richardson, "Climbing robot," U.S. Patent Application US2025/0091669A1, Mar. 20, 2025.
[5] INSPIRE UTC, Missouri S&T. (2021). *Steel Climbing Robot on Steel Column* [Video]. YouTube. https://www.youtube.com/watch?v=xFnUgWRm4PM
[6] Fang G, Cheng J. Advances in Climbing Robots for Vertical Structures in the Past Decade: A Review. Biomimetics (Basel). 2023 Jan 22;8(1):47.
[7] Keng Huat Koh, M. Sreekumar, S.G. Ponnambalam, Hybrid electrostatic and elastomer adhesion mechanism for wall climbing robot, Mechatronics, Volume 35, 2016, Pages 122-135
[8] Liu, J.-H., & Padrigalan, K. (2021). Design and Development of a Climbing Robot for Wind Turbine Maintenance. *Applied Sciences*, *11*(5), 2328.
[9] Parness, A., Frost, M., Thatte, N., King, J.P., Witkoe, K., Nevarez, M., Garrett, M., Aghazarian, H. and Kennedy, B. (2013), Gravity-independent Rock-climbing Robot and a

 © 2026 by CLIMBING CLANKERS

Sample Acquisition Tool with Microspine Grippers. J. Field Robotics, 30: 897-915.
[10] Noohi, E., Mahdavi, S. S., Baghani, A., & Ahmadabadi, M. N. (2010). Wheel-Based Climbing Robot: Modeling and Control. *Advanced Robotics*, *24*(8–9), 1313–1343.
[11] C. Sahakian, J. Idefort, J. Viera, and E. Laniesse, “Robot for tightening a series of bolt nuts on a vehicle chassis and manufacturing process,” U.S. Patent 11,851,122, Dec. 26, 2023.
[12] H. Nam, W. Choi, D. Ryu, Y. Lee, S. Lee and B. Ryu, "Design of a bolting robot for constructing steel structure," *2007 International Conference on Control, Automation and Systems*, Seoul, Korea, 2007, pp. 1946-1949.
[13] B. Chu, K. Jung, M. Lim, and D. Hong, “Robot-based construction automation: An application to steel beam assembly (Part I),” *Automation in Construction*, vol. 32, pp. 46–61, 2013.
[14] McMaster-Carr Supply Co., “6-Point Standard Socket, 1/2 in. Square Drive, 1/2 in. Size, Part No. 5545A13.” https://www.mcmaster.com/5545A13.
[15] “Coefficients of Friction,” *Engineers Edge*. https://www.engineersedge.com/coeffients_of_friction.htm.
[16] Sculpteo. (n.d.). *Pull-out resistance of threaded inserts: Testing and results*. Sculpteo. https://www.sculpteo.com/en/3d-learning-hub/design-guidelines/pull-out-resistance-of-threaded-inserts-testing-and-results/
[17] SEAS3D PLA Technical Data Sheet. (n.d.). *PLA technical data sheet*. SEAS3D.
[18] MatWeb. “Aluminum 6061-T6; 6061-T651.” www.matweb.com,www.matweb.com/search/DataSheet.aspx?MatGUID=b8d536e0b9b54bd7b69e4124d8f1d20a.

APPENDICES



Full_Robot_Code

© 2026 by CLIMBING CLANKERS